AIMS Materials Science, 13(3): 518–537.
DOI: 10.3934/matersci.2026025
Received: 11 March 2026
Revised: 20 May 2026
Accepted: 02 June 2026
Published: 09 June 2026

https://www.aimspress.com/journal/Materials

Research article

Experimental study on the mechanical properties of red clay stabilized by cement and multi-source solid wastes

Xunan Li*, Xiang Zhou and Michael Adeyemi

School of Civil Engineering, Xijing University, Xian, Shaanxi Province, 710123, China

* **Correspondence:** Email: lixunanxj@163.com; Tel: +86-153-5685-9585.

Abstract: Red clay exhibits unfavorable engineering properties that limit its direct use as subgrade fill material. This study investigated the stabilization of red clay using cement, fly ash, silica fume, and brick powder. Uniaxial compression tests were conducted on single-stabilizer and multi-component mixtures to evaluate their mechanical behavior. Results show that cement provides the highest strength improvement, followed by silica fume, fly ash, and brick powder. Multi-component mixtures with cement as the primary binder, combined with silica fume and fly ash, achieved the highest strengths from 2.0 to 2.4 MPa, representing a 40% increase over single-stabilizer treatments. Three distinct failure modes were identified: ductile fragmentation, X-shaped conjugate shear bands, and single-plane brittle shear. Their evolution is governed by the dominant stabilization mechanism. Range analysis revealed the influence weights of the four stabilizers on strength development as 0.594 for cement, 0.183 for silica fume, 0.135 for fly ash, and 0.088 for brick powder. A predictive model based on a comprehensive strengthening coefficient was proposed and validated against experimental data. The findings demonstrate that the synergistic use of cement and multi-source solid waste provides an effective approach for red clay improvement.

Keywords: red clay; multi-source solid waste; stabilization; uniaxial compression; failure mode

1. Introduction

In road engineering, red clay is often used as a subgrade fill material because it is widely available and can be sourced locally. However, this soil has problematic properties, including a high liquid limit [1–3], high shrinkage-swelling potential [3,4], and low bearing capacity [5]. Without treatment,

it typically fails to meet the required standards for subgrade fill in terms of strength, stability, and durability [6–8]. In the field, subgrades built with red clay are susceptible to uneven settlement, slope failure, and pavement damage under changing moisture and loading conditions [9]. These problems can significantly reduce the service life and safety of the road. For this reason, research into stabilizing red clay with additives is both essential for ensuring construction quality and safety and necessary for enabling road development in areas where red clay is prevalent.

Extensive experimental research has been conducted on the stabilization of red clay, with most studies focusing on conventional stabilizers such as cement [10–12] and lime [13–15]. Cement improves soil mechanical properties through hydration reactions that produce cementitious products, including C-S-H gel and ettringite [11]. These hydration products effectively fill soil pores and bond particles together, significantly enhancing the strength and stiffness of the stabilized clay [12]. Cement stabilization is a well-established and reliable technique, and it remains one of the primary solutions for red clay improvement. However, excessive cement content leads to increased soil brittleness and an abrupt transition from ductile to brittle failure, accompanied by rising construction costs [12]. Furthermore, the high energy consumption and carbon emissions associated with cement production have drawn increasing attention, posing a conflict with the principles of green and sustainable development. Lime is another conventional material used for soil stabilization. It operates through cation exchange, flocculation-agglomeration, and pozzolanic reactions [13]. It effectively reduces the plasticity of clay but exhibits slow strength development and carries a risk of strength loss when soaked. With industrial development, industrial by-products such as fly ash, blast furnace slag, and silica fume have gradually attracted research attention [14–16]. These materials offer both resource utilization value and performance improvement potential. Fly ash generates cementitious compounds through pozzolanic reactions during long-term curing, which enhances soil strength while enabling solid waste reuse [17]. However, its slow early strength development makes it difficult to meet the rapid construction requirements of engineering projects. Blast furnace slag is hydraulic, forming a cementitious system when activated by alkalis. Compared to fly ash, it gains strength more quickly in the early stages [18]. Nevertheless, its volume stability requires careful attention. Silica fume consists of ultrafine particles and has high pozzolanic activity. It fills micropores in the soil and improves density through secondary hydration [19]. However, its relatively high material cost limits large-scale application. While these materials have mitigated some shortcomings of conventional stabilizers, each industrial by-product still presents distinct performance drawbacks. This situation has motivated a shift in research focus toward multi-material stabilization approaches [20–22]. Existing studies have demonstrated that binary blended systems, such as cement–fly ash and cement–slag, can reduce cement consumption while maintaining strength development [23–25]. The cement–silica fume combination further optimizes soil compactness through micro-filling effects [26]. These findings provide a theoretical foundation for multi-component stabilization. While most existing studies have concentrated on binary mixtures, the synergistic mechanisms in ternary or higher-order systems remain poorly understood. As sustainability gains attention in geotechnical engineering, the use of multiple solid wastes for clay stabilization has become an attractive option. These materials contribute different functions, including binding, filling, and reactivity [27]. The combined use of cement and multiple solid wastes can enhance soil performance and enable waste valorization. However, multi-component stabilization involves more complex interactions among multiple factors than single-component or binary mixtures. Key issues, such as the individual contributions of the constituent materials, their relative influence weights, and their optimal dosage ranges, remain poorly understood. Existing studies

have focused primarily on comparing strength indices. Systematic analyses of stress–strain behavior and failure mode evolution are still lacking. Consequently, a comprehensive understanding of the mechanical behavior and failure mechanisms of multi-component-stabilized clay has not yet been established. Additionally, most investigations focused on single or binary stabilizer systems. As a result, synergistic mechanisms and quantitative contributions of multi-component systems that combine cement with various solid wastes remain insufficiently clarified. Also, failure modes are generally described only qualitatively, and the systematic links between macroscopic failure characteristics and microscopic mechanisms under multi-component stabilization have not been well established. Furthermore, few studies provide quantitative weight evaluations and physically interpretable strength prediction models for multi-source solid waste-stabilized red clay. These gaps impede the scientific design of mix proportions and the performance optimization of composite-stabilized red clay.

This study investigates the mechanical properties, failure modes, and stabilization mechanisms of red clay stabilized by cement and multi-source solid wastes, including fly ash, silica fume, and brick powder. Through uniaxial compression tests and range analysis, the strength characteristics and influence weights of different stabilizers are analyzed. The evolution of failure modes is systematically interpreted in conjunction with stabilization mechanisms, and a quantitative predictive model based on a comprehensive strengthening coefficient is established. The research results can provide a reliable experimental basis and a practical quantitative method for the design and application of multi-component-stabilized red clay in subgrade engineering.

2. Materials and methods

2.1. Experimental materials

The soil sample used in this study was collected from a subgrade construction site of an expressway in Yunnan Province, China. Its basic physical properties are summarized in Figure 1. The soil sample exhibits a continuous particle size distribution ranging from 10^{-4} to 1.0 mm, with fine particles (<0.075 mm) accounting for over 60% of the total mass, indicating a typical fine-grained soil composition. The soil has a specific gravity of 2.71, while its liquid limit, plastic limit, and plasticity index are 39.20%, 20.90%, and 18.4%, respectively. According to the test methods of soils for highway engineering (JTG 3430-2020) [28], the soil is classified as low-liquid-limit clay. Additionally, the optimum moisture content and maximum dry density of the soil are determined to be 16.3% and 1.68 g/cm^3, respectively, which provide critical baseline parameters for sample preparation and subsequent soil improvement experiments.

In this study, four types of stabilizers were employed for soil improvement, namely Portland cement (PC), fly ash (FA), silica fume (SF), and brick powder (BP). Specifically, Saima brand P.O 42.5 ordinary Portland cement was adopted as the cementitious material. Fly ash was collected from a thermal power plant located in Wuhan City, Hubei Province, China, while silica fume was supplied by Hubei Yunda Daye Co., Ltd. Brick powder was sourced from the demolition site of an old building in Hubei Province, China. The chemical compositions of these four stabilizers were determined by X-ray fluorescence spectrometry (XRF), and the detailed results are presented in Table 1. XRF analysis indicates that fly ash, silica fume, and brick powder are all aluminosilicate solid wastes with latent pozzolanic activity. Notably, fly ash contains a certain amount of CaO, which allows it to

generate a small quantity of $Ca(OH)_2$ independently. In contrast, silica fume and brick powder can only fully activate their pozzolanic reactivity by relying on $Ca(OH)_2$ produced from cement hydration.

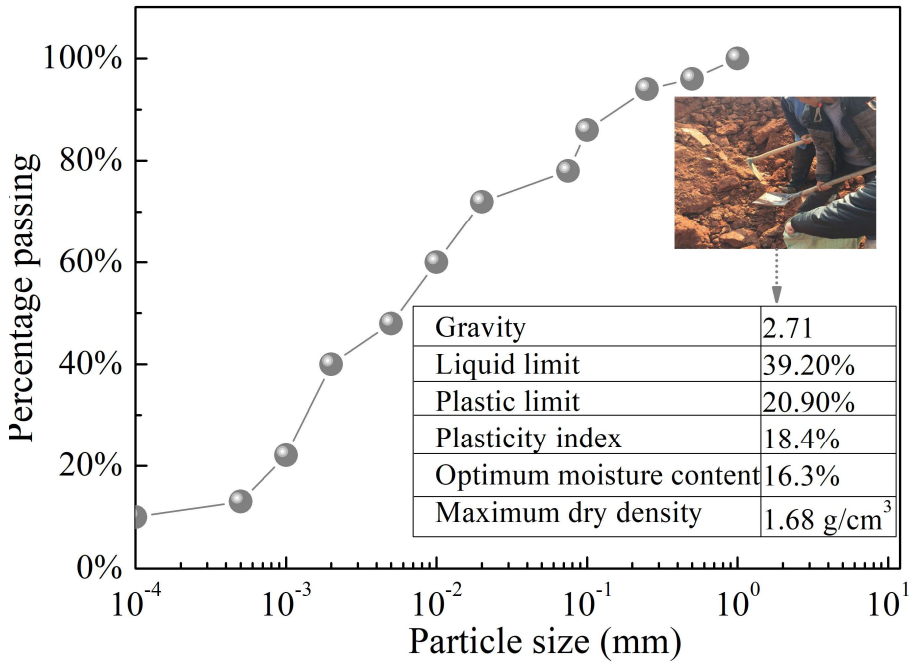

Figure 1. Basic properties of the soil sample.

Table 1. Chemical composition of stabilizers.

Stabilizers	Chemical composition								
	SiO_2	Al_2O_3	Fe_2O_3	CaO	K_2O	MgO	TiO_2	Na_2O	SO_3
Portland cement	23.80%	7.20%	3.96%	58.10%	0.95%	1.68%	--	0.32%	--
Fly ash	49.35%	19.50%	5.80%	7.60%	1.70%	2.05%	1.10%	1.35%	0.55%
Silica fume	89.65%	2.28%	0.72%	0.65%	2.85%	3.15%	0.07%	--	--
Brick powder	69.15%	19.28%	4.82%	0.73%	3.45%	1.44%	0.55%	0.58%	--

2.2. Experimental program and scheme

To comprehensively evaluate the mechanical responses of clay under different stabilizer proportions, three categories of tests, including composite stabilization, single-component stabilization, and a control group, were designed in this study. The multi-component mixture groups (S1–S16) were arranged as a uniformly spaced mixed-level design with reasonable and even dosage gradients. This arrangement aims to preliminarily explore the strength variation law, failure mode evolution, and synergistic characteristics of multi-component-stabilized red clay. For the composite stabilization scheme, composite tests were conducted with four factors, namely cement, FA, SF, and BP, to investigate the strength enhancement characteristics under the synergistic effects of multiple materials. The detailed experimental arrangement is presented in Table 2. Meanwhile, to clarify the individual stabilization effect of each material, single-variable tests were conducted for each of the four stabilizers to examine their respective influences on the mechanical properties of the clay. In addition, uniaxial

compressive strength tests were performed on undisturbed soil samples without any stabilizer as a blank control group, providing a baseline for quantitatively evaluating the improvement effects of different stabilization schemes and ensuring the scientific validity and comparability of the experimental results. To achieve both cost-effectiveness and satisfactory stabilization performance, the content of each stabilizer was controlled within 10%, based on existing research findings [29,30].

Table 2. Experimental scheme.

Sample	Soil stabilizer			
	Portland cement	Fly ash	Silica fume	Brick powder
S1	1%	1%	1%	1%
S2	1%	3%	3%	3%
S3	1%	5%	5%	5%
S4	1%	7%	7%	7%
S5	3%	1%	3%	5%
S6	3%	3%	1%	7%
S7	3%	5%	7%	1%
S8	3%	7%	5%	3%
S9	5%	1%	5%	7%
S10	5%	3%	7%	5%
S11	5%	5%	1%	3%
S12	5%	7%	3%	1%
S13	7%	1%	7%	3%
S14	7%	3%	5%	1%
S15	7%	5%	3%	7%
S16	7%	7%	1%	5%

In this study, all soil samples were prepared at their respective optimum moisture contents. The compaction degree was set to 0.9 to simulate the most unfavorable conditions, although the recommended value for subgrade construction is greater than 0.9. Prior to sample preparation, the soil was mixed with a predetermined amount of water and then sealed in plastic bags for 24 h to ensure uniform moisture distribution. Given the hydration effect of the stabilizers, these materials were added only after the moisture conditioning process and were thoroughly mixed with the soil. Cylindrical samples measuring 50 mm in height and 100 mm in diameter were subsequently prepared using the layered compaction technique. A constant curing period of 28 days was adopted for all samples, as the influence of curing time was beyond the scope of this investigation. The curing temperature was controlled at 25 ± 2 ℃, the relative curing humidity was maintained above 95%, and all specimens were taken out for mechanical tests after reaching the designed curing age of 28 days. After sample preparation, uniaxial compressive tests were conducted, as shown in Figure 2. The tests were performed using a YAW-300KN computer-controlled electronic pressure testing machine at a loading rate of 1.0 mm/min. Each group comprised three parallel samples, and the mean strength value was adopted as the representative result.

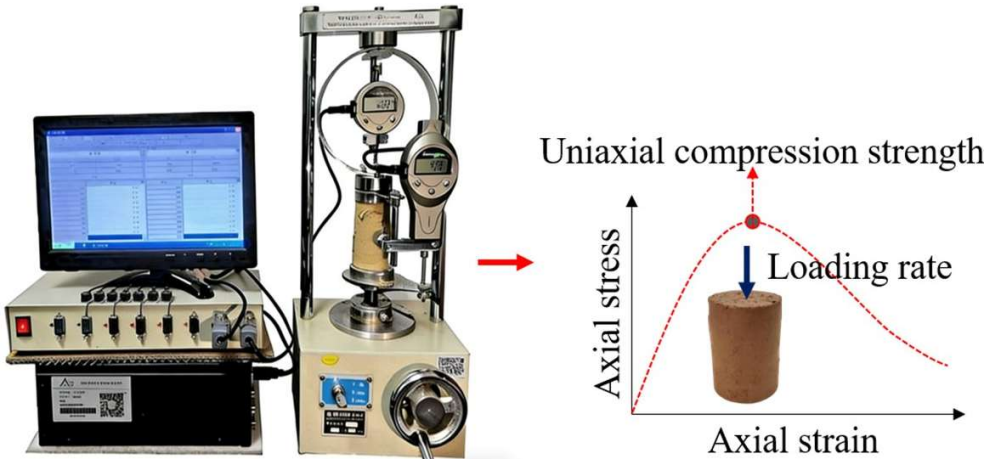

Figure 2. Uniaxial compression test system for stabilized soil samples.

3. Results and discussion

3.1. Uniaxial compression strength

Figure 3a–d presents the uniaxial compressive stress–strain relationships of soils stabilized with single additions of cement, fly ash, silica fume, and brick powder, respectively, at varying stabilizer contents. Figure 3e illustrates the stress–strain responses of soils subjected to multi-component mixing schemes S1 through S16. All samples exhibit typical strain-softening behavior, characterized by a rapid increase in axial stress to a peak value followed by a gradual decline toward a residual strength. This behavior is caused by the formation and gradual propagation of internal microcracks after the peak stress. With increasing axial strain, the cemented structure inside the soil is gradually damaged, resulting in the reduction of bearing capacity. Similar mechanical responses and damage mechanisms have been reported in stabilized red clay by Wang et al. [10] and Liu et al. [11], which confirms that the evolution law of stress and strain obtained in this study conforms to the general mechanical characteristics of stabilized soils. Regarding the effects of individual stabilizers, significant differences are observed in both the strengthening mechanisms and the magnitude of performance enhancement among the four materials. Cement (Figure 3a) and silica fume (Figure 3c), as highly reactive cementitious materials, generate stable hydration products that form cemented skeletons, resulting in the most substantial strength improvements. Notably, silica fume–stabilized soils exhibit slightly higher peak strengths and initial tangent moduli than their cement-stabilized counterparts. This advantage originates from the micro-filling effect and secondary hydration reactions of silica fume. Silica fume with ultra-fine particles fills the micropores between soil particles and cement hydrates and then reacts with calcium hydroxide to generate additional C-S-H gel. Pranav et al. [19] confirmed that silica fume improves soil density and strength through the above mechanisms, and the results in this study are consistent with their findings. Fly ash (Figure 3b) primarily contributes to strength development through pozzolanic reactions. Its early-age strength gain is relatively slow; consequently, at equivalent stabilizer contents, the peak strengths of fly ash–stabilized soils are lower than those achieved with cement or silica fume, though still significantly higher than that of the untreated reference soil. This difference is attributed to the slow pozzolanic reaction rate of fly ash. The activity of fly ash needs sufficient curing time to be fully mobilized, so its early strength development is

relatively slow. Cokca [23] reported the same slow strength development law in fly ash–stabilized clay, which is highly consistent with the performance observed in this study. Brick powder (Figure 3d), functioning as a recycled aggregate-based stabilizer, improves soil structure mainly through physical filling and particle interlocking. Among the four stabilizers, it yields the smallest strength enhancement and exhibits more pronounced plastic characteristics. This is because brick powder only plays a physical filling role and cannot provide effective chemical cementation. It improves the soil structure mainly by particle interlocking, so its strengthening effect is limited. This mechanism has been widely recognized in related studies, and the results of this study are consistent with this understanding. For all soils stabilized with single additives, as the stabilizer content increases from 1% to 7%, both the peak strength and initial elastic modulus exhibit continuous growth, while the axial strain corresponding to the peak strength progressively decreases. This trend indicates that increasing stabilizer content effectively enhances the cementation strength and structural density of the soil, facilitating a transition from plastic to brittle failure behavior. It is worth noting that soils stabilized with silica fume and cement demonstrate greater sensitivity to variations in stabilizer content, whereas those treated with brick powder are less affected, suggesting that physical stabilization mechanisms provide more consistent mechanical performance across different content levels. In the multi-component mixing schemes (S1–S16), the stabilization effect is further optimized. Compared with single-additive stabilization, the multi-component combinations achieve superior synergistic improvements in both strength and toughness. Among these, mixtures incorporating cement as the primary binder, supplemented by silica fume and fly ash (S13–S16), exhibit the highest peak strengths and initial elastic moduli. The excellent performance is attributed to the synergistic effect of cement hydration, silica fume micro-filling and secondary hydration, and fly ash pozzolanic reaction. Cement provides the main cementation skeleton, silica fume optimizes the microstructure, and fly ash supplements the long-term strength. Wang et al. [10] and Pranav et al. [19] also confirmed that such multi-component systems exert complementary advantages and achieve better mechanical performance than single stabilizers. In contrast, mixtures dominated by brick powder (S1–S4) display relatively limited strength enhancement and more ductile failure modes, indicating that physical filling remains the predominant mechanism in such systems. As the cement content increases from 1% to 7% in the multi-component schemes, the peak strength of the stabilized soils consistently increases, while the axial strain at peak strength gradually decreases, accompanied by a transition from ductile to brittle failure behavior. These observations confirm that cement content is the primary determinant of the mechanical performance of stabilized soils. By forming a stable skeleton of hydration products, cement substantially enhances both the load-bearing capacity and the brittle characteristics of the treated soil. Furthermore, the appropriate incorporation of silica fume and fly ash optimizes soil density and durability without compromising strength, thereby offering greater flexibility for performance regulation in engineering applications.

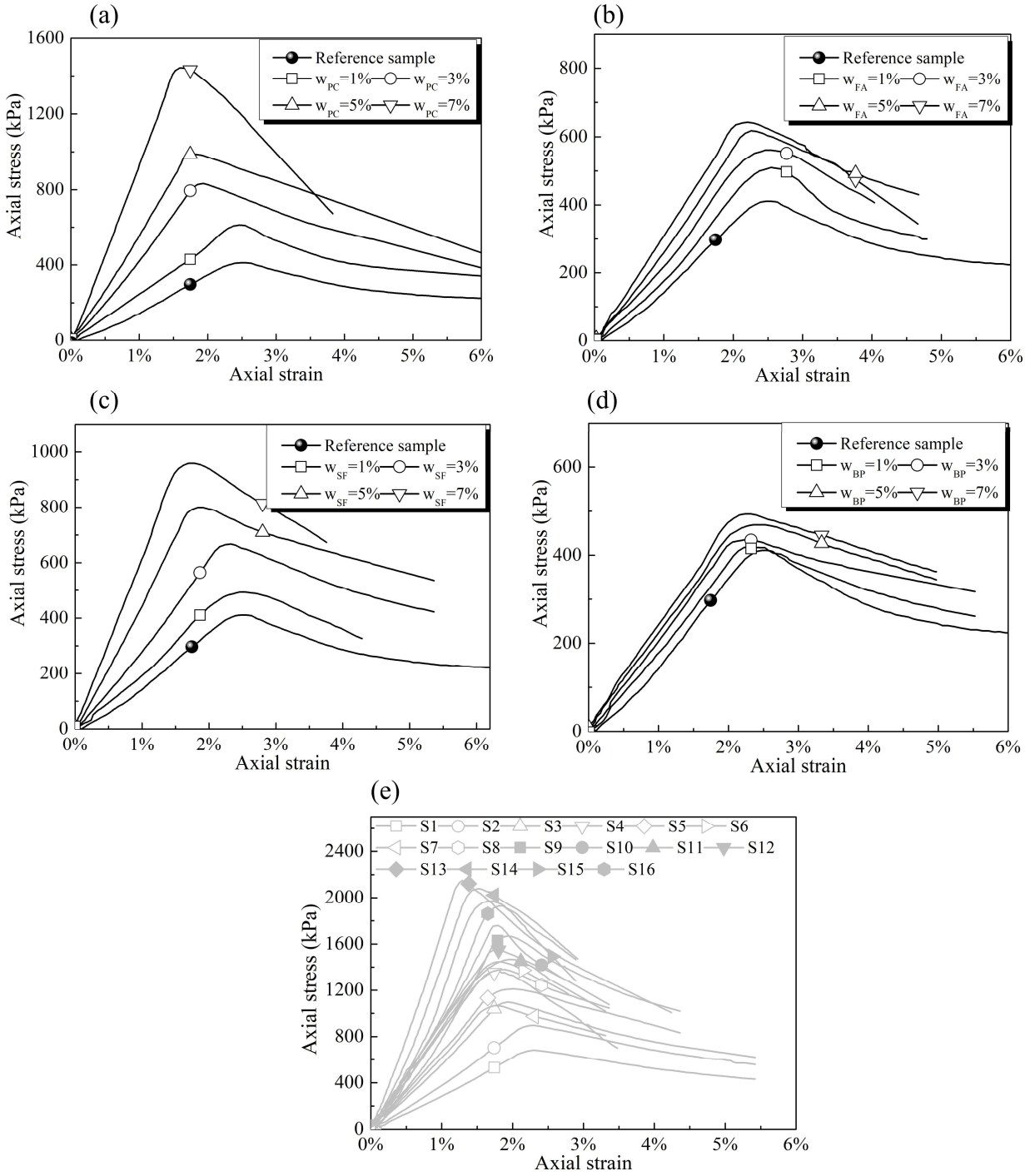

Figure 3. Stress–strain curves: (a) Portland cement; (b) fly ash; (c) silica fume; (d) brick powder; and (e) multi-stabilizer.

Based on the experimental results, the uniaxial compression strength values under different conditions are presented in Figure 4. Figure 4a shows the strength of soils stabilized with single stabilizers. For all four stabilizers, the uniaxial compression strength increases linearly with stabilizer content, but the strengthening effects differ significantly among them. Portland cement exhibits the highest strengthening efficiency. When the cement content increases from 1% to 7%, the uniaxial compression strength increases from approximately 0.4 to over 1.4 MPa. This improvement is attributed to the cementitious skeleton formed by hydration products, which enhances the soil's

load-bearing capacity. Silica fume shows the second-best performance. Its strength growth is slightly lower than that of cement, but remains considerably higher than that of fly ash and brick powder. This is because silica fume fills micropores and undergoes secondary hydration reactions, leading to a denser soil microstructure. Fly ash primarily relies on pozzolanic reactions, resulting in a relatively gradual strength increase. Brick powder, as a recycled material, mainly improves strength through physical filling and particle interlocking; therefore, its strength enhancement is the smallest among the four stabilizers. Figure 4b presents the uniaxial compression strength results for multi-component mixtures (S1–S16). The combinations containing cement as the primary binder, along with silica fume and fly ash (S11–S16), yield the highest strength values, ranging from 2.0 to 2.4 MPa. These values are significantly higher than those achieved with any single stabilizer. This superior performance results from the synergistic effects among cement hydration, silica fume filling and secondary reactions, and fly ash pozzolanic activity. Together, these mechanisms create a more compact and stable soil skeleton. In contrast, mixtures dominated by brick powder (S1–S4) exhibit relatively low strength values, indicating that physical filling alone provides limited strength improvement. It should be emphasized that this study only focuses on the uniaxial compressive strength under standard curing for 28 days. The improvement effects of stabilizers on Atterberg limits, shrinkage–swelling deformation, water stability, and long-term durability under complex environments are not involved. These indices are key for road performance evaluation of red clay subgrade and need to be further studied.

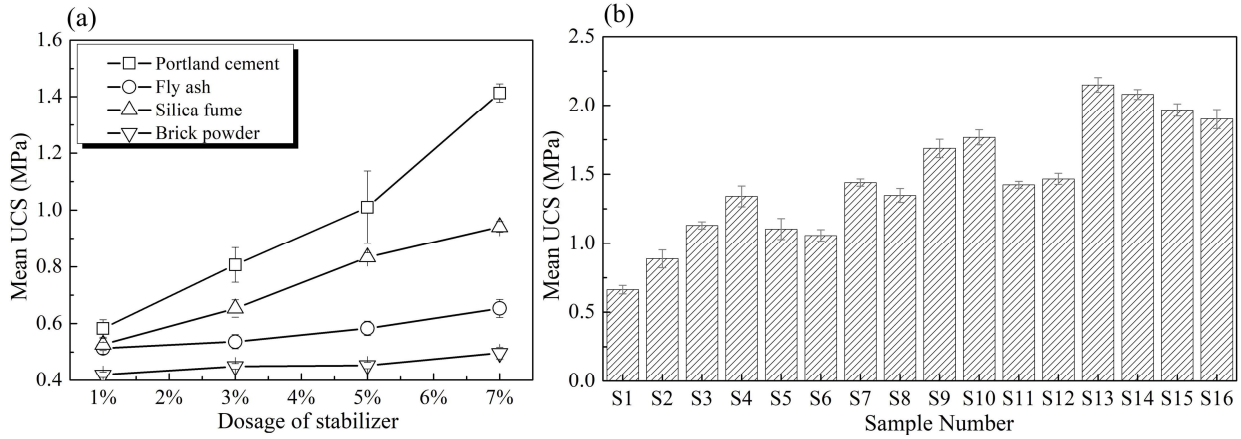

Figure 4. Uniaxial compression strength (UCS): (a) single-stabilizer conditions; and (b) multi-stabilizer conditions.

To further explore the microscopic essence of strength enhancement and mechanical property evolution of stabilized red clay revealed by macroscopic tests, scanning electron microscopy tests were conducted on typical samples, and the observed microscopic morphology is displayed in Figure 5. Observing the overall structural characteristics in Figure 5a at 1000× magnification, it can be found that the original scattered red clay particles are closely connected by massive hydration products. The structural transformation from particle contact support to cementitious material cementation support constitutes the core reason for the obvious improvement of uniaxial compressive strength and initial elastic modulus of modified soil. With the increase of cementitious stabilizer dosage, the amount of generated internal hydration products increases continuously, the internal pore volume of soil is effectively reduced, and the overall structure tends to be dense and rigid, which is consistent with the changing trend of mechanical parameters reflected in stress–strain curves.

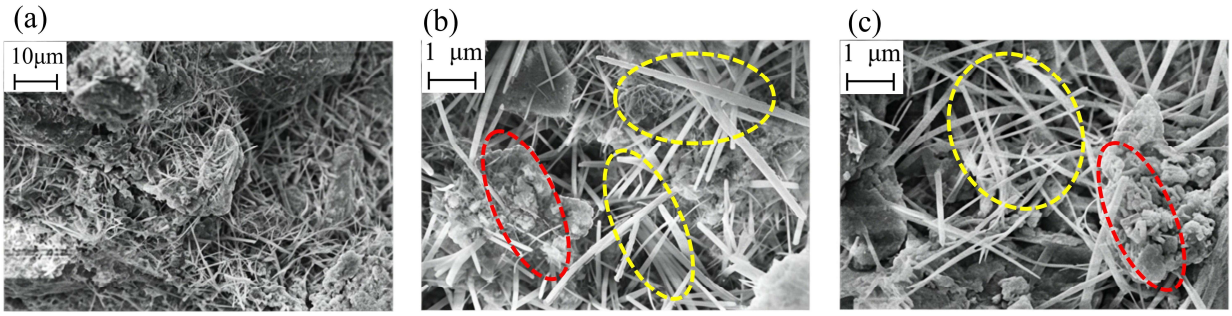

Figure 5. Scanning electron microscope (SEM) images at different magnifications: (a) low magnification (1000×); (b) high magnification (10000×) for region 1; and (c) high magnification (10000×) for region 2.

From the high-resolution images in Figure 5b,c at 10000× magnification, two typical microscopic structural forms can be clearly distinguished in combination with the marked areas. The needle-shaped and prismatic crystalline substances marked by yellow circles are the typical cement hydration product, ettringite. Such crystalline substances are mutually interwoven inside the soil to form a stable spatial skeleton structure, which can significantly improve the overall stiffness and load-bearing performance of soil samples. This microscopic strengthening mechanism has been fully confirmed in the existing research results of cement-based stabilized soil [10,11]. The regional structures marked by red circles show that red clay particles and recycled solid waste fillers, such as fly ash and brick powder, are tightly wrapped and bonded by amorphous calcium silicate hydrate gel. The cementation effect of gel substances integrates discrete soil particles into an integrated whole, further optimizes the internal compactness of the soil, and improves structural stability, which is in line with the microscopic filling and cementation improvement mechanism summarized in relevant studies [19]. There is a clear inherent logical correlation between microscopic structural differences and macroscopic mechanical behaviors. The fully developed interlaced ettringite crystal structure and continuously distributed cementing gel can reasonably explain why stabilized soil presents high peak strength and strong structural rigidity in uniaxial compression tests and gradually evolves toward brittle failure characteristics. When the internal cementation skeleton is completely formed, the soil sample has low peak strain and prominent brittleness, and it is easy to cause penetrating shear failure along a fixed weak surface. On the contrary, soil samples with insufficient hydration products and loose internal structures possess larger peak strain and lower strength level and show typical ductile failure features. This evolutionary law of mechanical properties is also consistent with the research conclusions reported in previous literature [11]. Moreover, microscopic morphological characteristics can sufficiently reflect the synergistic improvement effect among various stabilizers. Cement undertakes the main hydration reaction and constructs the primary cementation skeleton inside the soil matrix. Silica fume and fly ash can undergo a secondary pozzolanic reaction to supplement cementitious products, fill tiny internal pores, and optimize pore gradation. Recycled brick powder mainly optimizes soil particle grading and enhances the embedding occlusion effect between particles. This multi-dimensional synergistic modification effectively improves the compactness and uniformity of stabilized soil structure; this combined modification mechanism has also been widely recognized and verified in the field of composite-stabilized soil research [19,23]. In summary, the microscopic observation results are highly consistent with macroscopic mechanical test laws and inferred stabilization mechanisms, all of which provide reliable direct microscopic evidence for clarifying the

internal improvement principle of multi-component composite-stabilized red clay and verifying the scientific rationality of mix proportion design.

3.2. Failure mode

Figure 6 illustrates three typical failure modes of stabilized soils observed during uniaxial compression tests. The failure mode is closely related to the internal cementation strength, structural density, and crack propagation path. Relevant research shows that the transformation of failure modes in stabilized soil is controlled by critical conditions. Literature results indicate that key factors include cement content, peak strain, brittleness index, internal cementation strength, and structural compactness [31,32]. Higher cement content and better hydration effect will increase the cementation strength of soil samples. The failure mode will change from ductile fragmentation to brittle shear failure when the cementation strength reaches a certain critical level. Samples with weak cementation and loose structure tend to show ductile failure characteristics [31,32]. It should be noted that most existing studies on stabilized soil failure modes mainly adopt qualitative classification based on macroscopic morphology, and relevant quantitative indices, such as peak strain, brittleness index, softening modulus, and energy dissipation, have been proposed in recent literature to further distinguish failure characteristics [31,32]. According to Wang et al. [10] and Liu et al. [11], the failure characteristics of stabilized soil can directly reflect the strengthening mechanism and structural state. The three failure modes identified in this study are highly consistent with those reported in previous literature. Mode I (Figure 6a) is characterized by multiple non-penetrating fine cracks on the sample surface, with no distinct shear band formation, ultimately resulting in fragmented failure. This mode is predominantly observed in samples stabilized with brick powder alone. Since brick powder improves soil structure only through physical filling and particle interlocking, the cementation between soil particles remains weak. Under axial loading, micro-cracks initiate and propagate randomly in multiple directions, preventing the formation of a concentrated shear plane and exhibiting pronounced ductile failure characteristics. This type of failure is typically associated with insufficient interparticle bonding and relatively low structural integrity, as verified in earlier research [32]. Mode II (Figure 6b) displays X-shaped conjugate shear band failure, where the sample is divided into four parts by two intersecting primary shear bands. This mode represents the typical failure pattern of multi-component-stabilized soils. In composite systems with cement as the primary binder and silica fume and fly ash as supplementary materials, a dense and isotropic cemented skeleton forms within the soil. Under peak loading, stress concentrates and redistributes simultaneously in multiple directions, eventually developing conjugate shear bands. This mode reflects the mechanical characteristics of multi-component-stabilized soils, which combine high strength with good energy dissipation capacity. The occurrence of such a failure mode reflects moderate cementation strength and relatively uniform internal structure [31]. Mode III (Figure 6c) exhibits single-plane shear failure, where the sample splits along a penetrating shear band with a relatively smooth fracture surface. This mode is mainly observed in soils stabilized with highly reactive cementitious materials such as cement or silica fume alone. These stabilizers form a rigid load-bearing skeleton through hydration products. Under axial loading, stress concentrates intensely along a single potential shear plane. When the shear stress exceeds the soil's shear strength, brittle failure occurs along this plane, with the shear band inclination matching the internal stress field distribution. In summary, as the stabilization mechanism transitions from physical filling to cementitious hydration and further to multi-component synergistic cementation, the

failure modes of stabilized soils evolve accordingly from ductile fragmentation to brittle single-plane shear failure and, finally, to conjugate shear band failure. This evolutionary pattern provides an experimental basis for optimizing soft soil stabilization schemes and for preventing and controlling engineering failure risks.

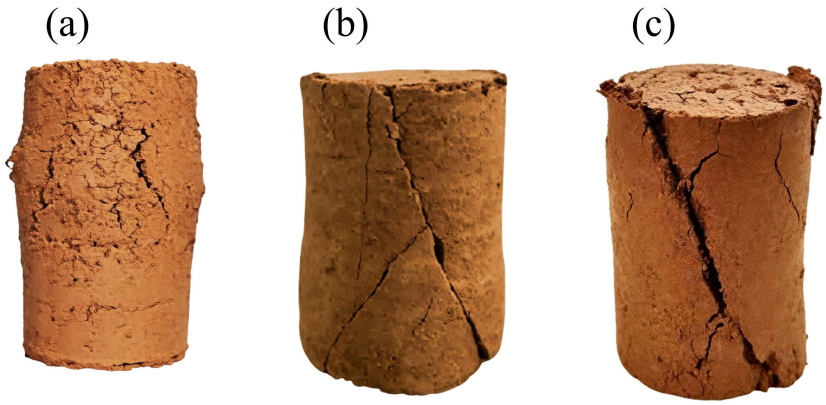

Figure 6. Typical failure modes: (a) Mode I; (b) Mode II; and (c) Mode III.

Figure 7 presents the statistical distribution of three typical failure modes observed in uniaxial compression tests of stabilized soils under single-stabilizer and multi-component mixing conditions. As shown in Figure 7a, under single-stabilizer conditions, the evolution of failure modes is closely related to the type and content of the stabilizer. For Portland cement and silica fume, as the content increases from 1% to 7%, the failure mode gradually transitions from Mode I to Mode II. This indicates that increasing the content of cementitious materials effectively enhances the cementation strength and structural density of the soil, leading to a transition from ductile to brittle failure behavior. In contrast, soils stabilized with fly ash or brick powder predominantly exhibit Mode I failure. Even at higher stabilizer contents, only a few samples display Mode II. This is attributed to the relatively slow early-age strength gain from fly ash pozzolanic reactions and the primarily physical filling effect of brick powder. Neither material is capable of forming a sufficient cementitious skeleton to induce brittle failure. Figure 7b presents the statistical results of failure modes observed under multi-component mixing schemes (S1–S16). Compared with single-stabilizer conditions, multi-component combinations significantly alter the distribution of failure modes. As the cement content increases in the mixing schemes, the occurrence of Mode II and Mode III increases notably, while the proportion of Mode I decreases accordingly. In particular, combinations using cement as the primary binder, supplemented by silica fume and fly ash (S13–S16), predominantly exhibit Mode II and Mode III failures. This suggests that multi-component synergistic stabilization not only enhances soil strength but also improves post-failure energy dissipation capacity, resulting in more complex and stable failure patterns. By contrast, combinations dominated by brick powder (S1–S4) remain characterized mainly by Mode I failure, indicating that physical filling still plays a dominant role in such systems, and that the potential for strength enhancement is limited. The type, content, and combination ratio of stabilizers are key factors governing the failure modes of stabilized soils. Under the conditions of this study, the synergistic stabilization scheme using cement as the primary binder, supplemented with silica fume and fly ash, effectively induces more complex and stable failure patterns. The transition between different failure modes is closely regulated by the development level of the internal cementation skeleton. Enhanced cementation and improved compactness alter the stress distribution

and crack propagation path within the material. Such variations eventually lead to the transformation of failure modes, as supported by published findings [10,31,32].

(a)

I	I	I	III	I	I	I	II	I	I	II	I	II	I	I	I
I	I	III	III	I	II	II	I	I	I	III	III	I	I	I	I
I	II	II	III	I	I	II	II	I	II	I	II	I	II	I	I
1%	3%	5%	7%	1%	3%	5%	7%	1%	3%	5%	7%	1%	3%	5%	7%
Portland cement				Fly ash				Silica fume				Brick powder			

(b)

I	I	I	I	I	I	I	II	II	II	II	I	II	II	II	III
I	II	II	II	I	I	II	II	II	II	III	III	III	III	III	III
II	I	I	III	I	II	I	II	II	III	II	II	III	II	III	II
S1	S2	S3	S4	S5	S6	S7	S8	S9	S10	S11	S12	S13	S14	S15	S16

Figure 7. Typical failure modes: (a) single-stabilizer conditions; and (b) multi-stabilizer conditions.

3.3. Mathematical model

To quantitatively elucidate the influencing laws and the relative importance of different stabilizer dosages on the mechanical properties of clay, a range analysis was systematically employed to process the experimental results. Since the current experimental design is a uniformly spaced mixed-level design rather than a standard orthogonal design, range analysis is adopted to determine the influence weight and primary–secondary order of each stabilizer, which can provide a reliable basis for evaluating the contribution of each component in the multi-component system. The average value of all corresponding test results for the *i*-th factor at the *j*-th level is expressed as Eq 1:

$$\bar{\sigma}_{ij} = \frac{1}{n_j} \sum_{t=1}^{n_j} \sigma_{ijt} \tag{1}$$

where $\bar{\sigma}_{ij}$ is the average value of the uniaxial compression strength for the *i*-th factor at the *j*-th level; n_j denotes the number of test replicates corresponding to the *j*-th level; and σ_{ijt} represents the measured value of the mechanical property index for the *t*-th test under the *i*-th factor at the *j*-th level.

For the *i*-th factor, the range value is calculated using Eq 2:

$$R_i = max(\bar{\sigma}_{ij}) - min(\bar{\sigma}_{ij}) \tag{2}$$

where R_i is the range value of the *i*-th factor, which reflects the amplitude of variation in the test results caused by the level changes of the factor. A larger R_i value indicates a more significant effect of the factor's level variation on the mechanical properties of clay, meaning that the factor is more dominant in the improvement system.

The influence weight of each factor was calculated based on the range results, realizing a normalized evaluation of the relative importance of multiple factors. This weight index (g_i) eliminates

the dimensional difference between different ranges and can directly reflect the hierarchical order of each stabilizer in the composite stabilization system. The calculation formula is given as Eq 3:

$$g_i = \frac{R_i}{\sum R_i} \tag{3}$$

Based on the experimental results and the range analysis, the influence weights of four stabilizers on the mechanical properties of stabilized soils are shown in Figure 8. Cement exhibits the highest influence weight at 0.594, indicating its dominant role in the stabilization system as the core factor governing the strength and mechanical behavior of the treated soil. This finding aligns with the strengthening mechanism of cement, which functions as a highly reactive cementitious material that forms a stable cemented skeleton through hydration reactions. Silica fume ranks second, with an influence weight of 0.183. This is closely associated with its micro-aggregate filling effect and secondary hydration reactions, both of which contribute to optimizing the soil microstructure and enhancing the compactness and strength of the stabilized soil. Fly ash follows with an influence weight of 0.135, playing a supplementary role in the stabilization system through pozzolanic reactions that moderately improve soil performance. Brick powder exhibits the lowest influence weight at 0.088, reflecting the relatively limited capacity of its physical filling and particle interlocking mechanisms to regulate the mechanical properties of the soil. As such, it primarily functions as an auxiliary filling material in the stabilization system. The influence weights of the stabilizers are closely correlated with their respective mechanisms of action. Cementitious stabilizers (cement and silica fume) demonstrate significantly greater control over the performance of stabilized soils compared to physical filling-type stabilizers (brick powder). These findings provide valuable weighting references for the design of multi-component stabilization schemes, suggesting that priority should be given to ensuring adequate content of core cementitious materials such as cement, supplemented by auxiliary materials like silica fume and fly ash, to achieve optimal stabilization outcomes. In addition, limited by the overall arrangement of the current experimental scheme, the test groups are not designed in accordance with standard factorial design principles. The obtained experimental data cannot meet the basic requirements for conducting an analysis of variance and significance verification based on principal component analysis. For this reason, this study only adopts range analysis to finish preliminary sorting of influencing factors, and fails to conduct an in-depth quantitative evaluation of the interactions between various influencing factors.

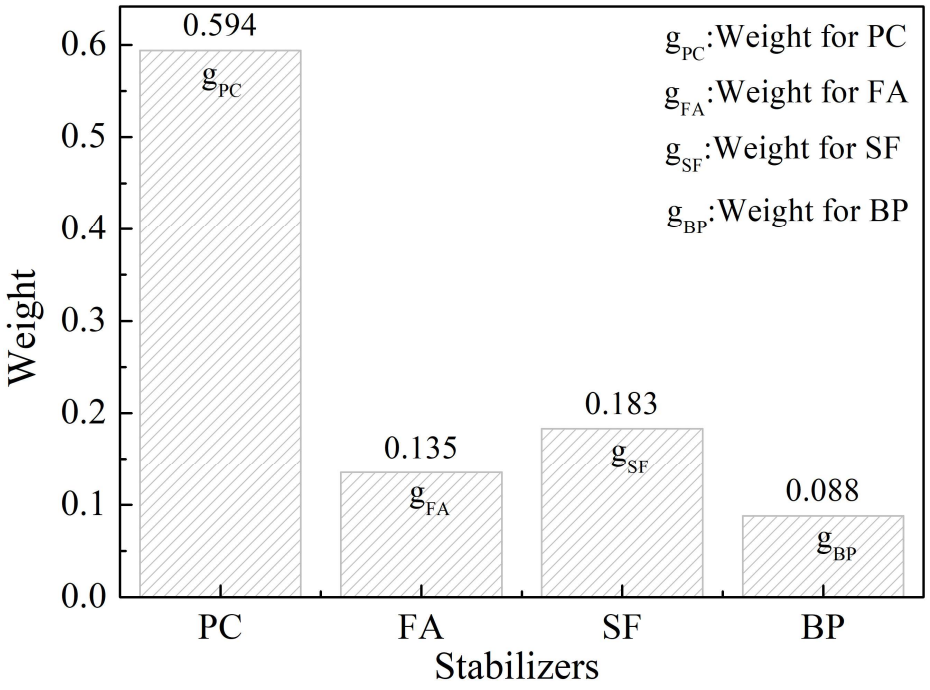

Figure 8. Weight distribution of different stabilizers.

Based on the weight characteristics of each factor mentioned above, a comprehensive strengthening coefficient ($G = g_{PC}w_{PC} + g_{FA}w_{FA} + g_{SF}w_{SF} + g_{BP}w_{BP}$) was further established in this study. Using the proposed comprehensive strengthening coefficient, the relationship between the normalized strength of improved soil and the comprehensive strengthening coefficient under different conditions was analyzed and is presented in Figure 9. It can be observed from the figure that the normalized strength exhibits an obvious linear relationship with the comprehensive strengthening coefficient, which can be expressed by Eq 4:

$$\sigma^N = \frac{\sigma - \sigma^R}{\sigma^R} = kG,\ with\ G = g_{PC}w_{PC} + g_{FA}w_{FA} + g_{SF}w_{SF} + g_{BP}w_{BP} \tag{4}$$

where σ^R represents the uniaxial compressive strength of the reference soil sample, and k is a model parameter that can be obtained by regression analysis. In this study, the value of k is determined as 69.312 based on the regression analysis results. It should be clearly stated that the proposed predictive model is established based on the experimental data of the multi-component-stabilized red clay system involved in this study, and its applicable scope is restricted to the tested mix proportion range of each stabilizer. The model is suitable for the composite stabilization system composed of cement, silica fume, fly ash, and brick powder with the dosage ranges adopted in this research. Beyond this mix proportion range or when other types of stabilizers are added, the model parameters need to be recalibrated through additional experiments to ensure the accuracy of performance prediction.

Based on Eq 4, the uniaxial compressive strength of stabilized soil with any stabilizer mix proportion can be determined, allowing for effective prediction of soil strength. To further verify the reliability of the proposed model, a series of laboratory uniaxial compression tests were performed on stabilized soil samples with various stabilizer contents. The comparison between the experimental results and the model predictions is illustrated in Figure 10. It can be seen that the predicted values are

in good agreement with the measured data. Accordingly, the proposed model can effectively characterize the strength behavior of stabilized soil under different stabilizer combinations and can provide a theoretical reference for the efficient evaluation of stabilized soil strength in future studies.

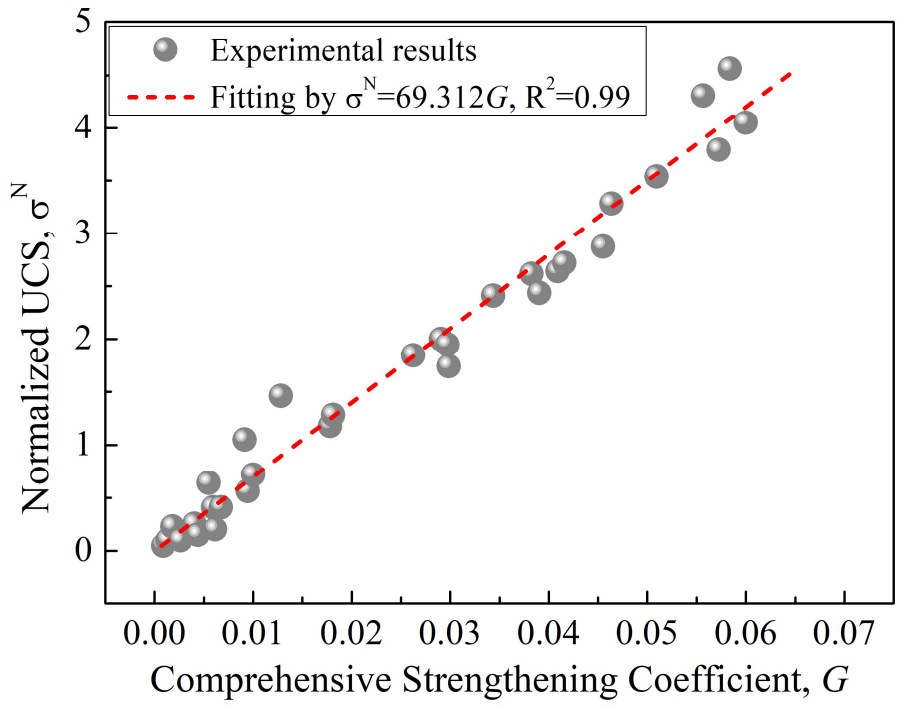

Figure 9. Relationship between the comprehensive strengthening coefficient and normalized uniaxial compression strength.

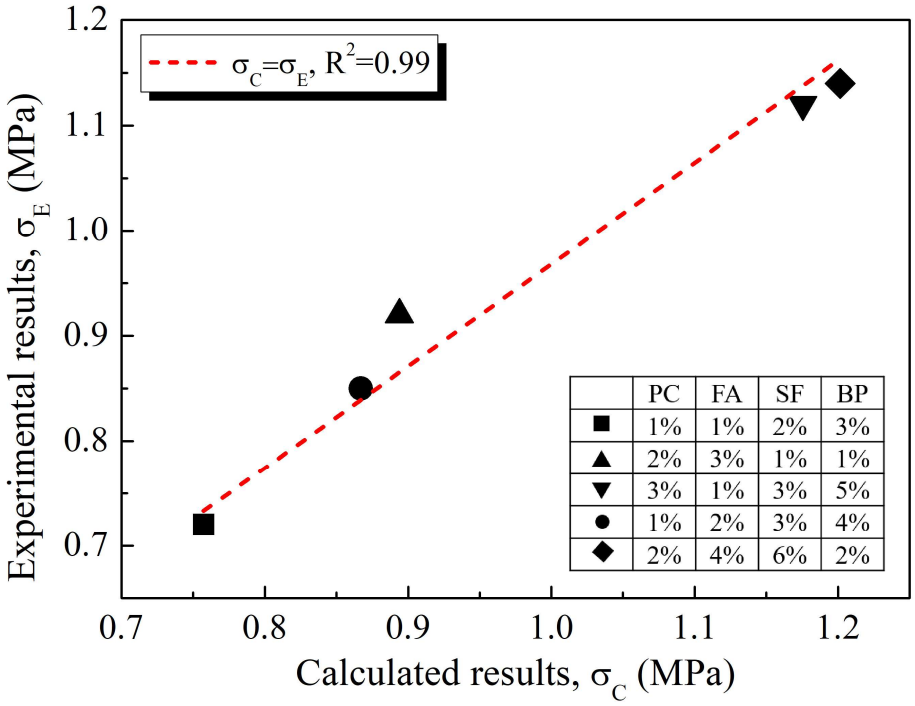

Figure 10. Comparison between calculated and experimental UCS.

4. Conclusions

Based on the experimental investigations and analyses presented in the preceding sections, the following conclusions can be drawn regarding the mechanical behavior of red clay stabilized with cement and multi-source solid wastes:

(1) The type and dosage of stabilizers greatly affect the strength of stabilized red clay. Cement exhibits the best reinforcing effect in single-component treatment, followed by silica fume, fly ash, and brick powder. With dosages rising from 1% to 7%, cement and silica fume can increase unconfined compressive strength beyond 1.4 MPa. The combined system of cement, silica fume, and fly ash achieves the optimal strengthening effect, with strength ranging from 2.0 to 2.4 MPa, 40% higher than specimens modified by a single stabilizer. This method effectively improves soil performance and realizes solid waste resource recycling.

(2) Three typical compression failure modes are classified for stabilized red clay. Different material action mechanisms dominate sample failure behaviors. Multi-component synergistic modification can form stable X-shaped conjugate shear failure, which enables the modified soil to maintain high strength and improve energy dissipation capacity. This conclusion provides a clear reference for regulating soil deformation performance in real-life engineering.

(3) Quantitative range analysis confirms that cement has the largest influence weight on soil strength, followed sequentially by silica fume, fly ash, and brick powder. A physical-based strength prediction model is established according to such influence rules. The predicted results show great consistency with experimental data, which can support rapid mix proportion design and strength evaluation of multi-component-stabilized red clay.

This research mainly focuses on short-term mechanical properties and failure characteristics of stabilized red clay. Some key road performance indicators, including plasticity, shrinkage and swelling properties, water stability, and environmental durability, are not considered in this work. Relevant systematic research will be carried out in follow-up studies to supply more comprehensive theoretical support for practical engineering promotion and application.

Use of AI tools declaration

The authors declare they have not used Artificial Intelligence (AI) tools in the creation of this article.

Acknowledgments

This work was supported by the Shaanxi Provincial Natural Science Foundation (Grant No. 2024JM518) and Xijing University, Xi'an, Shaanxi Province (Grant No. XJ0598).

Author contributions

Xunan Li: conceptualization, methodology, formal analysis, writing–original draft, supervision; Xiang Zhou: data curation, experiment operation, investigation; Michael Adeyemi: resources, writing–review & editing, language polishing.

Conflict of interest

The authors declare no conflict of interest.

References

1. Sun Y, Yu C, Jiang S, et al. (2025) Disintegration behaviors of red clay under wet-dry cycles. *JRMGE* 17: 5875–5892. https://doi.org/10.1016/j.jrmge.2024.09.005
2. Luo XW, Lu Z, Zhang JB, et al. (2024) Study on performance of geocell-reinforced red clay subgrade. *Geosynth Int* 31: 968–980. https://doi.org/10.1680/jgein.23.00068
3. Li LY, Zhang QS, Cao WQ, et al. (2024) Model tests on red clay foundation reinforced by coir geotextiles. *J Mater Civ Eng* 36: 06024002. https://doi.org/10.1061/JMCEE7.MTENG-16717
4. Souhassou H, Fahoul Y, El-Mrabet I, et al. (2024) Optimization of basic red 29 dye removal onto a natural red clay using response surface methodology. *J Iran Chem Soc* 21: 275–291. https://doi.org/10.1007/s13738-023-02924-5
5. Wang X, Wu B, Cui K, et al. (2024) A modified critical state model and its application in Haikou red clay, In: Hazarika H, Haigh SK, Chaudhary B, et al. *Natural Geo-Disasters and Resiliency. IC-CREST 2023. Lecture Notes in Civil Engineering*, Singapore: Springer. https://doi.org/10.1007/978-981-99-9223-2_35
6. Liu BC, Zhou HF, Wang XB, et al. (2024) Effect of modifiers on the disintegration characteristics of red clay. *Sustainability* 16: 4551. https://doi.org/10.3390/su16114551
7. Gu C, Sun Q, Zhang L, et al. (2024) Effect of temperature on the radon release characteristics of red clay. *J Environ Radioact* 280: 107565. https://doi.org/10.1016/j.jenvrad.2024.107565
8. Wang ZY, Sun Q, Geng JS, et al. (2025) Fracture pattern and damage characteristics of red clay under freezing effects. *Eng Fract Mech* 327: 111468. https://doi.org/10.1016/j.engfracmech.2025.111468
9. Zhao FT, Liu J, Wang Y, et al. (2024) Dynamic mechanical properties of unsaturated red clay subjected to impact loading, In: Wang S, Huang R, Azzam R, et al. *Engineering Geology for a Habitable Earth: IAEG XIV Congress 2023 Proceedings, Chengdu, China. IAEG 2023. Environmental Science and Engineering*, Singapore: Springer. https://doi.org/10.1007/978-981-99-9057-3_39
10. Wang MY, Li MD, Dai RH, et al. (2024) Mechanical properties of tire chip and cement stabilised red clay. *Geomech Geoeng* 19: 868–878. https://doi.org/10.1080/17486025.2024.2324876
11. Liu Y, Chen K, Jian H, et al. (2024) Road properties of cement-phosphogypsum-red clay under dry and wet cycles. *PLoS ONE* 19: e0314276. https://doi.org/10.1371/journal.pone.0314276
12. Ding JW, Wan X, Jiao N, et al. (2024) Collaborative effects of red mud and phosphogypsum on geotechnical behavior of cement-stabilized dredged clay. *Bull Eng Geol Environ* 83: 200. https://doi.org/10.1007/s10064-024-03699-6
13. Zhao XS, Deng Q, Yang QJ, et al. (2025) Study on compressive strength characteristics of lime-fly ash composite improved mottled red clay. *Arab J Geosci* 18: 145. https://doi.org/10.1007/s12517-025-12285-3
14. Aqel R, Attom M, El-Emam M, et al. (2024) Piping stabilization of clay soil using lime. *Geosciences* 14: 122. https://doi.org/10.3390/geosciences14050122

15. Govindasamy P, Taha MR (2024) Changes in chemical concentration of silty clay added with lime and nanolime, In: Ismail A, Zulkipli FN, Mohd Daril MA, et al. *Engineering Frontiers*, Cham: Springer. https://doi.org/10.1007/978-3-031-56844-2_9
16. Oloimutie JP, Nzimbi PK (2025) Mechanical and microstructural properties of clay tile waste concrete treated with silica fume. *Adv Mater Sci Eng* 15: 4341855. https://doi.org/10.1155/amse/4341855
17. Almuaythir S, Zaini MSI, Hasan M (2025) Shear strength, compressibility, and consolidation behaviour of expansive clay soil stabilized with lime and silica fume. *Sci Rep* 15: 26185. https://doi.org/10.1038/s41598-025-10642-6
18. Joyklad P, Suriwong T, Inyai T, et al. (2024) Environmentally friendly binders from calcium carbide residue and silica fume and feasibility for soft clay stabilization. *Case Stud Constr Mat* 20: e03117. https://doi.org/10.1016/j.cscm.2024.e03117
19. Pranav S, Tyagi G, Lahoti M, et al. (2025) Novel lime-silica fume-modified limestone calcined clay cement (LC3) binder system for sustainable pavement construction. *Clean Techn Environ Policy* 27: 6433–6448. https://doi.org/10.1007/s10098-025-03284-9
20. Meng C, Yang W, Ren XJ, et al. (2023) In-situ soil texture classification and physical clay content measurement based on multi-source information fusion. *Int J Agr Boil Eng* 16: 203–213. https://doi.org/10.25165/j.ijabe.20231601.6918
21. Feng LX, Zhao ZF, Yang HY, et al. (2025) Clay-hosted lithium exploration in the Wenshan region of Southeastern Yunnan Province, China, using multi-source remote sensing and structural interpretation. *Minerals* 15: 826. https://doi.org/10.3390/min15080826
22. Kusniadi W, Apriyanti Y, Sandy BDA (2024) The effect of adding fly ash on the shear strength of clay soil considering the age of fly ash. *IOP Conf Ser Earth Environ Sci* 1419: 012006. https://doi.org/10.1088/1755-1315/1419/1/012006
23. As M, Cokca E (2025) Stabilization of an expansive clay containing sulfate with Soma fly ash. *Arab J Geosci* 18: 170. https://doi.org/10.1007/s12517-025-12315-0
24. Raja K, Sampathkumar V, Anandaraj S, et al. (2024) Comparative study on stabilisation of Bentonite clay using municipal incinerated bottom ash and fly ash, In: Reddy KR, Ravichandran PT, Ayothiraman R, et al. *Recent Advances in Civil Engineering. ICC IDEA 2023. Lecture Notes in Civil Engineering*, Singapore: Springer. https://doi.org/10.1007/978-981-99-6229-7_30
25. Pittman R, Hu B, Webster K (2021) Improvement of soil property mapping in the great clay belt of northern Ontario using multi-source remotely sensed data. *Geoderma* 381: 114761. https://doi.org/10.1016/j.geoderma.2020.114761
26. Ma R, Guo LP, Sun W, et al. (2025) Well-dispersed silica fume by surface modification and the control of cement hydration. *Adv Civ Eng* 2018: 6184105. https://doi.org/10.1155/2018/6184105
27. Uddin MA, Bashir MT, Khan AM, et al. (2024) Effect of silica fume on compressive strength and water absorption of the Portland cement–silica fume blended mortar. *Arab J Sci Eng* 49: 4803–4811. https://doi.org/10.1007/s13369-023-08204-x
28. JTG 3430-2020 (2020) Test methods of soils for highway engineering. Bejjing, China: Highway Science Research Institute and Ministry of Communications. ISBN 9787114168284.
29. Wu H, Gao J, Liu C, et al. (2024) Reusing waste clay brick powder for low-carbon cement concrete and alkali-activated concrete: A critical review. *J Clean Prod* 449: 141755. https://doi.org/10.1016/j.jclepro.2024.141755

30. Sengul T, Akray N, Vitosoglu Y (2023) Investigating the effects of stabilization carried out using fly ash and polypropylene fiber on the properties of highway clay soils. *Constr Build Mater* 400: 132590. https://doi.org/10.1016/j.conbuildmat.2023.132590
31. Li ZS, Zhang YN, Janiszewski M, et al. (2022) Radial deformation and failure of stabilised soft clay under uniaxial compression. *Soils Found* 62: 101213. https://doi.org/10.1016/j.sandf.2022.101213
32. Erarslan N, Aliha MRM (2025) Fracture and damage analysis of cement-stabilized fine and coarse grain soils under static and cyclic loading using chevron-notched SCB specimen. *Fatigue Fract Eng Mater Struct* 48: 2708–2724. https://doi.org/10.1111/ffe.14598

AIMS Press